
ParA encoded on chromosome II of *Deinococcus radiodurans* binds to nucleoid and inhibits cell division in *Escherichia coli*

VIJAYA KUMAR CHARAKA, KRUTI P MEHTA and HS MISRA*

Molecular Biology Division, Bhabha Atomic Research Centre, Mumbai 400 084, India

*Corresponding author (Fax, +91-22-25505151; Email, hsmisra@barc.gov.in)

Bacterial genome segregation and cell division has been studied mostly in bacteria harbouring single circular chromosome and low-copy plasmids. *Deinococcus radiodurans*, a radiation-resistant bacterium, harbours multipartite genome system. Chromosome I encodes majority of the functions required for normal growth while other replicons encode mostly the proteins involved in secondary functions. Here, we report the characterization of putative P-loop ATPase (ParA2) encoded on chromosome II of *D. radiodurans*. Recombinant ParA2 was found to be a DNA-binding ATPase. *E. coli* cells expressing ParA2 showed cell division inhibition and mislocalization of FtsZ-YFP and those expressing ParA2-CFP showed multiple CFP foci formation on the nucleoid. Although, *in trans* expression of ParA2 failed to complement SlmA loss *per se*, it could induce unequal cell division in *slmAminCDE* double mutant. These results suggested that ParA2 is a nucleoid-binding protein, which could inhibit cell division in *E. coli* by affecting the correct localization of FtsZ and thereby cytokinesis. Helping *slmAminCDE* mutant to produce minicells, a phenotype associated with mutations in the 'Min' proteins, further indicated the possibility of ParA2 regulating cell division by bringing nucleoid compaction at the vicinity of septum growth.

[Charaka VK, Mehta KP and Misra HS 2013 ParA encoded on chromosome II of *Deinococcus radiodurans* binds to nucleoid and inhibits cell division in *Escherichia coli*. *J. Biosci.* **38** 487–497] DOI 10.1007/s12038-013-9352-5

1. Introduction

Cell division in bacteria occurs through the regulated functions of a large number of cell division proteins forming divisome complex (Adams and Errington 2009; Erickson *et al.* 2010). The formation of FtsZ ring, a component of divisome, is temporally and spatially regulated where DNA replication, genome segregation and positioning of nucleoid in the cells play key regulatory roles (Lutkenhaus 2007). In some bacteria, the spatial regulation of FtsZ is brought about by mechanism of nucleoid occlusion manifested by proteins such as 'Noc' protein in *Bacillus* (Wu and Errington 2004) and 'SlmA' in *E. coli* (Tonthat *et al.* 2011), and the inhibition of Z-ring formation at its vicinity has been demonstrated. Molecular mechanisms underlying the regulation of cell division and divisome assembly in response to environmental stresses are less understood in bacteria. However, it has been shown that the SOS response protein such as Sula in *E. coli* (Norman *et al.* 2005) and YneA in *Bacillus subtilis* (Kawai *et al.* 2003) could inhibit bacterial cell division in response to DNA

damage. The Sula functions by directly interacting with FtsZ and by inhibiting its GTPase activity (Dajkovic *et al.* 2008). The classical SOS response mechanisms to DNA damage, as known in most of the bacteria (Walker 1996), has been reported to be absent in *D. radiodurans* (Narumi *et al.* 2001).

D. radiodurans is characterized for its extreme resistance to different abiotic stresses including radiations and desiccation (Battista 2000). An efficient DNA double-strand break (DSB) repair (Blasius *et al.* 2008; Zahradka *et al.* 2006) and a strong oxidative stress tolerance (Slade and Radman 2011) are amongst the various mechanisms that contribute to the robustness of this organism. The accumulation of Mn²⁺ complexes of small metabolites (Daly *et al.* 2004) and synthesis of different types of antioxidant metabolites such as carotenoids (Tian and Hua 2010) and pyrroloquinoline quinone (PQQ) (Rajpurohit *et al.* 2008) are implicated in its strong oxidative stress tolerance and for protecting its proteome from oxidative damage. Earlier, the roles of PQQ in oxidative stress tolerance of both mammalian cells and bacterial system have been demonstrated *in vivo*

Keywords. Cell division; *Deinococcus*; genome segregation; nucleoid-binding protein; ParA; Walker-type ATPase

Supplementary materials pertaining to this article are available on the *Journal of Biosciences* Website at <http://www.ias.ac.in/jbiosci/sep2013/supp/Charaka.pdf>

(Misra *et al.* 2012). *D. radiodurans* harbours four genetic elements designated as chromosome I, chromosome II, megaplasmid and a small plasmid (White *et al.* 1999). Genome sequence analysis shows that chromosome I primarily encodes the majority of proteins required for normal growth of this bacterium (Makarova *et al.* 2001). The chromosome II and megaplasmid encode proteins mostly known for their roles in secondary functions including stress response mechanisms. Chromosome I and chromosome II contain one putative *parAB* operon each, while megaplasmid contains two putative *parAB* operons (White *et al.* 1999). The ParAs and ParBs have been annotated on the basis of amino acid sequence similarities, the occurrence of unique functional domains, and positions on these genetic elements and their expression in form of dicistronic operon. In addition, these elements also encode proteins with Walker-type ATPase domain similar to small ParAs. However, the roles of such proteins in genome segregation and/or otherwise in bacteria containing multipartite genomes are not well studied. *D. radiodurans* cells treated with γ radiation exhibit the longer lag phase, the period that witnesses the efficient DSB repair and is a prerequisite for the commencement of cell division (Cox and Battista 2005). Therefore, the regulation of cell division and genome segregation in *D. radiodurans* exposed to extensive DNA damage became interesting to understand. While characterizing the ParA2 (ParA of chromosome II) roles in genome segregation of *D. radiodurans*, we observed that unlike other recombinant proteins excluding FtsZ, expressed in *E. coli*, the ParA2 expression in *E. coli* leads to cell elongation. Here we elucidate the molecular mechanisms underlying ParA2 inhibition of cell division in *E. coli*. The cells expressing ParA2 showed a concentration-dependent increase in cell length, which was found to be due to mislocalization of FtsZ-YFP throughout the elongated cells of *E. coli*. These cells showed ParA2-CFP foci formation on nucleoid, and an increase in the number of such foci was observed with the increase in cell length. ParA2 was shown to be a DNA-binding ATPase, and its inhibition to FtsZ ring formation was not due modulation of its GTPase activity and/or sedimentation characteristics. In spite of this, ParA2 could complement SlmA loss in *slmA*AminCDE double mutant and showed no cellular lethality in γ -type cells lacking SlmA. These results suggested that ParA2 is a DNA-binding protein that localizes on the nucleoid *in vivo* and alters FtsZ localization pattern and cell division, possibly by posing nucleoid obstruction at the vicinity of septum growth.

2. Methods

2.1 Bacterial strains and materials

The *D. radiodurans* R1 strain ATCC13939 a generous gift from Dr M Schaefer, Germany (Schaefer *et al.* 2000), was maintained in TGY (0.5% Bacto Tryptone, 0.3% Bacto Yeast Extract, 0.1% Glucose) broth or on agar plate as required at 32°C. *E. coli*

expression vector pET28a(+) (Novagen Inc), pAMCYAN (Clontech Inc) and pLAU85 (pBAD *fisZYFP:lac I* CFP) (Lau *et al.* 2003), and their derivatives were maintained in *E. coli* strain DH5 α in presence of kanamycin (25 μ g/ml) and ampicillin (100 μ g/mL), respectively. Other recombinant techniques used were as described in (Sambrook and Russell 2001). All the molecular biology grade chemicals including restriction enzymes and DNA modifying enzymes were purchased from Sigma Chemical Company, USA, Roche Biochemicals, Germany, New England Biolabs, USA, and Bangalore Genie, India.

2.2 Bioinformatic analysis

The Functional motif search and structure prediction studies were carried out as described earlier (Das and Misra 2011), using standard online bioinformatics tools. In brief, the amino acid sequence of DRA0001 annotated as putative ParA was subjected to a PSI-BLAST search with the SWISS-PROT database with 'genome-partitioning proteins' as keywords. After five iterations, the sequences obtained were aligned by CLUSTAL-X, for conserved motifs search. The sequences of close homology were aligned by T-COFFEE and the conserved motifs were marked. Secondary structure was inferred from PSIPRED, JNET and Prof at the Quick2D server at Max-Planck Institute for Developmental Biology.

2.3 Construction of expression plasmids

Genomic DNA of *D. radiodurans* R1 was prepared using protocols as published previously (Battista *et al.* 2001). The ORF DR_A0001 encoding putative ParA type protein on chromosome 2 (ParA2) of *D. radiodurans*, was PCR amplified from genomic DNA of bacterium using A001F (5'GGAATTCATATGATGGTG AGCGCTGTGA3') and A001R (5'CCGCTCGAGTCATGCGTTTTCCCGGGA3') primers incorporated *NdeI* and *XhoI* sites respectively at the 5' ends of the primers. PCR product was cloned at *NdeI-XhoI* sites in pET28a (+) to yield pETA2. For making CFP translation fusion, the *drA0001* was PCR amplified using forward primer A2F (5'CCCAAGCTTGATGGGCAGCAGCAGCCATCAT3') and reverse primer A2R (5'CGGGATCCATTGCGTTTTCCCGGGA3') having *HindIII* and *BamHI* sites incorporated at the 5' of respective primers. PCR product was cloned at *HindIII* and *BamHI* sites in pAMCYAN (Clontech Laboratories, Inc) to yield pA2CFP. The pETA2 was transformed into *E. coli* BL21 (DE3) pLysS for the expression of recombinant protein while pA2CFP was transformed into both *E. coli* JM109 and AB1157 as required. The inducible expression of recombinant ParA2 was confirmed by SDS-PAGE and ParA2-CFP by immunoblotting using GFP antibodies using manufacturer protocols (Clontech Laboratories, Inc.).

2.4 Expression and purification of recombinant protein

The recombinant ParA2 protein of *D. radiodurans* expressing on pETA2 in transgenic *E. coli* BL21 (DE3) pLysS was purified by nickel-affinity chromatography using modified protocols as described earlier (Kota *et al.* 2010). In brief, the isopropyl β -D-1-thiogalactopyranoside (IPTG) induced cell pellet was directly suspended in Cell Lytic Express (Sigma Chemical Company, USA) and incubated at 37°C for 1h with mild agitation. Lysate was centrifuged at 15000g for 30 min and the pellet containing majority of the recombinant protein into the inclusion bodies was separated from clear supernatant. Pellet was dissolved in buffer B containing 100 mM NaH₂PO₄, 10 mM Tris-HCl, pH 8.0 and 8 M urea. Mixture was incubated at room temperature for 30 min and centrifuged at 12000g for 20 min. The recombinant protein was purified from clear supernatant using protocols described earlier (Kota *et al.* 2010). The eluted fractions were checked on SDS-PAGE and refolded by serial dilution of urea with concurrent increase of DTT concentration. The fractions showing near to homogeneity in ParA2 preparation were pooled and dialysed in buffer containing 20 mM Tris-HCl, 50mM NaCl, 1 mM DTT, 1 mM EDTA, 1mM PMSF and 50% glycerol. The protein was stored in small aliquots at -20°C for subsequent uses. The mass spectrometric analysis of ParA2 proteins was carried out commercially (The Centre for Genomic Applications, New Delhi). The peptide mass fingerprints of recombinant polypeptide matched with ParA2 encoding from chromosome 2 of *D. radiodurans* and ensured homogeneous preparation.

2.5 DNA protein interaction studies

For DNA binding activity assay of ParA2 protein, the 284 bp putative BS3-type centromeric sequence of chromosome I (Charaka and Misra 2012) was PCR-amplified from genomic DNA from *D. radiodurans* using forward primer (5'AGAA CCAGCCCGACTGGA 3') and reverse primer (5' ACAGGAT GCAC TCGTAACT 3'). DNA was purified from gel (QIAGEN Inc., Germany) and labelled at 3' end with dig-dUTP (Roche Biochemicals, Germany) following manufacturers protocols. Approximately 10 pmol of labelled substrate was incubated with increasing concentration of protein (200–1000 ng) at 37°C for 20 min in a 20 μ L reaction mixture containing 50 mM HEPES, pH8.0, 100 mM NaCl, 5 mM MgCl₂, 30 mM Na-Acetate. Mixtures were separated on 5% native PAGE and Digoxigenin-labelled DNA probe was immunoblotted with anti-digoxigenin-AP antibodies (Roche Biochemicals, Germany) and signals were detected using NBT/BCIP (Roche Biochemical) colour reagent using the manufacturer's protocol.

2.6 Measurements of ATPase and GTPase activities

ATPase activity of recombinant ParA2 was checked using a modified protocol as described in (Kota *et al.* 2010). In brief,

the increasing concentrations of ParA2 (0.05 to 4 μ g) were incubated with and without DNA, in reaction mixture containing 50 mM HEPES pH 8.0, 100 mM NaCl, 5 mM MgCl₂, 30 mM Na-acetate and 1 mM ATP, for 20 min at 37°C. The reaction was stopped using malachite green reagent. The release of Pi from ATP was measured at 630 nm and Pi concentration was estimated using standard procedure as described in (Geladopoulos *et al.* 1991). ATPase activity was calculated as nanomoles Pi formed per min/mg protein. For studying the effect of ATP and dsDNA on ATPase activity of ParA2, the dsDNA was pre-incubated with ParA2 and then incubated with ATP for different time period and assayed as described above. GTPase activity of FtsZ was measured as the release of Pi from GTP and estimated as described above. In brief, ~2 μ M purified recombinant FtsZ was incubated with 1mM GTP for 1 h at 37°C in reaction mixture containing 50 mM HEPES, pH 7.2, 50 mM KCl and 5 mM MgCl₂. The reaction was stopped with malachite green reagent and release of inorganic Pi was measured as described above. For studying the effect of ParA2 on GTPase activity of FtsZ, the above reaction mixture was incubated with FtsZ, with and without 2 μ M ParA2, 100 ng DNA and 1mMATP as required. The DNA, ATP, ParA2 and FtsZ controls were processed in parallel under identical conditions.

2.7 Expression of ParA2-CFP and FtsZ-YFP and fluorescence microscopic studies

E. coli cells harbouring pA2CFP were grown in presence of ampicillin (100 μ g/mL), and those harbouring pETA2 and pLAU85 together, were grown in LB supplemented with Kan (25 μ g/mL) and ampicillin (100 μ g/mL) overnight and inducible expression of recombinant proteins on pA2CFP and pETA2 was achieved with 200 μ M IPTG while on pLAU85 with 0.005% arabinose using standard protocols. Expression of recombinant proteins was confirmed by immunoblotting using respective antibodies as described earlier (Misra *et al.* 2006). Fluorescence microscopy of *E. coli* cells were carried out as described in (Weiss *et al.* 1999) using Zeiss AxioImager (Carl Zeiss) equipped with Zeiss AxioCam MRm camera. In brief, the *E. coli* cells were induced with 200 μ M IPTG for 4h before every fluorescence microscopic experiments were conducted. *E. coli* BL21 expressing ParA2 with and without FtsZ-YFP and *E. coli* AB1157 expressing ParA2-CFP and ParA1 separately were analysed under fluorescence microscope. In brief, the 5 μ L cells expressing these proteins in different combinations were mounted onto 1% agarose coated slide and pictures were taken on Axio Imager M1 Fluorescence Microscope (Carl Zeiss). The images were analyzed by using Axiovision 4.8 Rel software. Final image preparation was done using Adobe Photoshop CS3 software. Cell length measurements were done using Axiovision 4.8 software, data was analysed and plotted using Graph pad prism.

3. Results

3.1 *ParA2* was a DNA-binding ATPase

Multiple sequence alignment of ParA2 with other ParA-type proteins using CLUSTAL X program showed that ParA2 contains the typical A, A' and B components of Walker motifs that are found in P-loop ATPases (figure 1A). Unusually, it was found that ParA2 is missing one of the largely conserved lysine at the beginning of the Walker A motif, which was also conserved in ParA encoded on chromosome I of *D. radiodurans* (DrParA1). Phylogenetic analysis indicated that ParA2 is evolutionarily different from other chromosomal type ParAs including ParA1 of *D. radiodurans* (figure 1B) and it was placed between chromosomal type ParAs and other small ATPases involved in regulation of bacterial cell division. ParA2 showed considerable identity with the cell division regulatory proteins at amino acid levels. Recombinant ParA2 was purified (supplementary figure 1) and its identity was further confirmed by mass spectrometry (data not given). The purified ParA2 showed both DNA binding (figure 2A) and ATPase activities (figure 2B). The DNA binding efficiency of ParA2 increased further in the presence of ATP, and its ATPase activity was stimulated with DNA. These results suggested that ParA2 is evolutionarily different from other bacterial ParAs and is a DNA-binding ATPase. Increase in dsDNA binding activity of ParA2 in the presence of ATP and the concentration-dependent increase in ATPase-specific activity indicated the cooperative binding of this protein interaction with DNA, and therefore, ParA2 binding with bacterial nucleoid could be hypothesized.

3.2 *ParA2* binds to nucleoid and inhibits cell division in *E. coli*

ParA2-CFP was expressed in *E. coli* AB1157 on pA2CFP plasmid (supplementary figure 2) and cells were examined under fluorescence microscope. Results showed cell elongation and localization of multiple spots of ParA2-CFP on false blue-coloured DAPI-stained nucleoid spread throughout the cell (figure 3). Since chloramphenicol treatment was used for studying genome condensation in *E. coli* (Zusman *et al.* 1973), the cells expressing ParA2 were treated with chloramphenicol and the localization of ParA2-CFP on the condensed nucleoid was ascertained (figure 3). These results indicated that ParA2 colocalizes with nucleoid in *E. coli*. Effect of ParA2 on growth and cell division was monitored in *E. coli*. Transgenic *E. coli* expressing ParA2 showed a significant reduction in colony-forming units (CFU) as compared to untransformed cells and the cells expressing ParA1 (figure 4) on multicopy plasmid (Charaka and Misra 2012). ParA2 expressing in *E. coli* JM109, a *recA* minus host, showed similar effects as that of ParA2 expressing in *E. coli* AB1157 (data not shown). Nearly no effect in optical density at 600 nm while several-fold decrease in CFU in

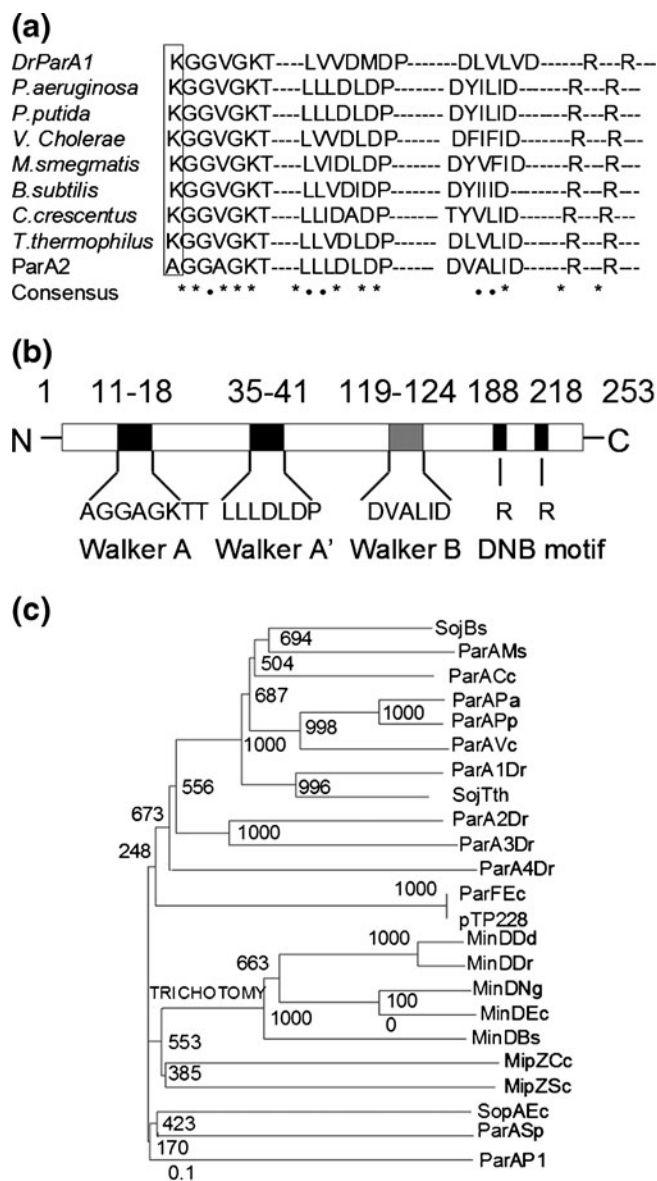


Figure 1. Functional motifs search in the putative ParA-type protein of chromosome II (ParA2) in *Deinococcus radiodurans*. Amino acid sequence of ParA2 was searched for homology with other related proteins in database. Multiple sequence alignment (MSA) of ParA2 with ParA1 of *D. radiodurans* (DrParA1) and other bacterial proteins having Walker-type motifs showed the presence of Walker A and A', Walker B motifs and DNA-binding motifs (A). Position of respective boxes in ParA2 is shown in schematic representation (B). Closeness of ParA2 with its relatives was determined and shown in phylogenetic tree (C). MSA of ParAs from *D. radiodurans* (identified with suffix Dr) were aligned with ParA, MinD and MipZ proteins of other bacteria available in the database and identified with a suffix of first letters of their genus followed by species.

the cells expressing ParA2 could be attributed to the continued increase in cell volume but inhibition of the cytokinesis. This

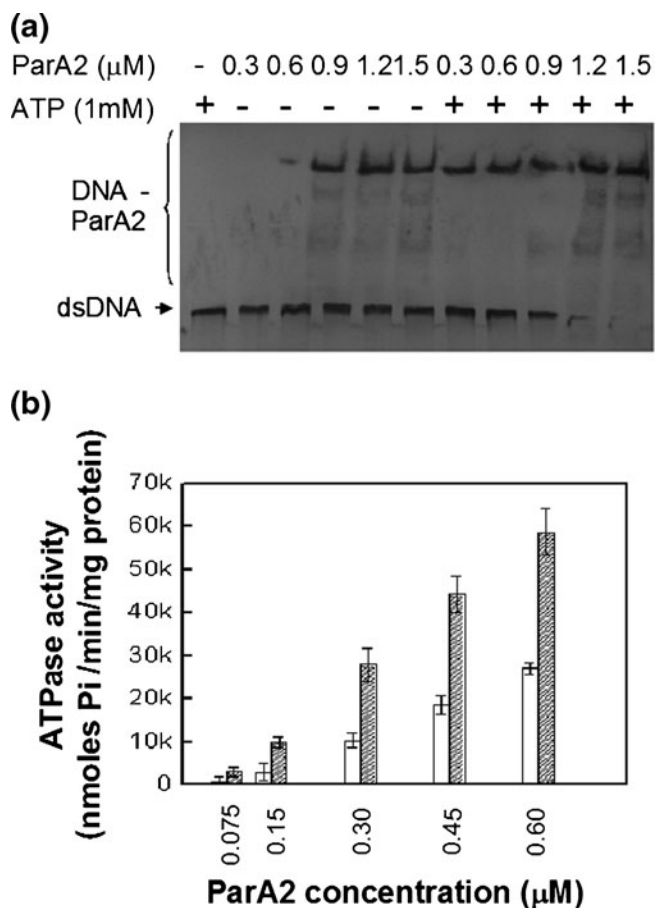


Figure 2. *In vitro* activity characterization of recombinant ParA2. The 284 bp long dsDNA was purified and labelled at 3' end using DIG labelling kit. The $\sim 0.5 \mu\text{M}$ DIG-labelled DNA probe was incubated with increasing concentration of purified ParA2 (0.3 μM to 1.5 μM) in binding buffer (50 mM HEPES, 100 mM NaCl pH 8.0, 5 mM MgCl_2 , 30 mM Na-acetate) for 20 min at 37°C and then separated by 5% native PAGE. DNA was transferred to nylon membrane and DIG-labelled DNA detected using anti-DIG antibody conjugated with alkaline phosphatase (A). ATPase activity of ParA2 was determined with increasing concentration of protein in absence (open box) and presence (filled box) of dsDNA (B).

indicated that ParA2 is most likely affecting cell division in *E. coli*. Effect of cell division inhibition on cell elongation was further monitored microscopically. As expected, the number of cells showing cell elongation increased on longer induction with IPTG (figure 5). Cells harbouring expression vector and those expressing another recombinant protein ParA1 as control did not show cell elongation (figure 5A) at least up to 6 h post IPTG treatment. After 9 h post IPTG induction, nearly 80% of the cells expressing ParA2 were more than 2 μm in size as against the cells harbouring only vector or not making ParA2, where nearly 95% of the cells were less than 2 μm in size (figure 5B). Over-expression of FtsZ on plasmid did not rescue the ParA2

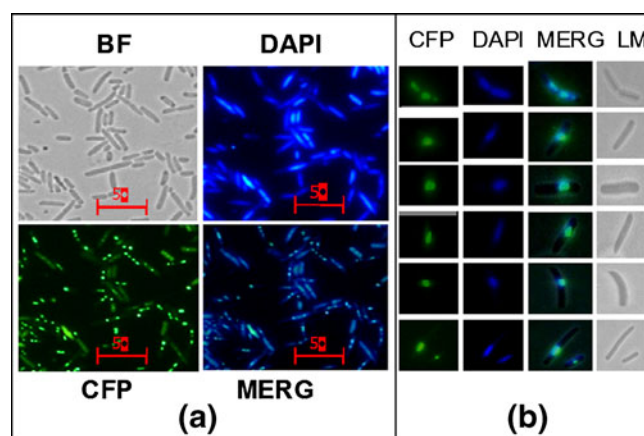


Figure 3. Localization of recombinant ParA2 in *E. coli* cells. *E. coli* AB1157 harbouring pA2CFP were induced with 100 μM IPTG for 4 h. Cells were collected and treated with 2 μL DAPI (2 mg/mL) and imaged under bright field (BF) and under DAPI fluorescence (DAPI) and CFP fluorescence (CFP). These cells were also treated with chloramphenicol (100 $\mu\text{g}/\text{mL}$) for 1 h and imaged as mentioned above. These images were superimposed (Merg) for locating the ParA2-CFP foci position in *E. coli* cells.

effect in ParA2 over-expressing *E. coli* cells (data not given). These results suggested that the increase in cell length and decrease in CFU per mL of cells expressing ParA2 seems to be due to ParA2 affecting cell division in *E. coli*.

3.3 ParA2 affected proper localization of FtsZ

In order to understand the mechanism of ParA2 inhibition of cytokinesis, the effect of ParA2 on FtsZ localization was monitored in recombinant *E. coli* BL21 co-expressing both ParA2 under T7 promoter and FtsZ-YFP under *araBAD* promoter on pLAU85 plasmid (Lau *et al.* 2003). Since over-expression of *E. coli* FtsZ is known to affect cell division, which eventually leads to cell elongation, the levels of FtsZ-YFP expression under P_{araBAD} was deliberately kept at a minimum to avoid the FtsZ-YFP transgenesis effect on cell elongation. Subsequently, the level of total FtsZ (FtsZ + FtsZ-YFP) in cells with and without ParA2 was determined and found to be same (supplementary figure 3). Cells expressing FtsZ-YFP alone showed a false-yellow-colour dense spot at the mid cell position while those harbouring pETA2 (ParA2 expression under T7 promoter) and pLAU85, but were induced with only arabinose, showed complete FtsZ ring formation in most of the cells as seen in control. When these cells were induced with both IPTG and arabinose for expressing both ParA2 and FtsZ-YFP concurrently, nearly 90% of the cells were exceptionally long and FtsZ-YFP mislocalization was observed throughout the elongated cells (figure 6). The relative position of FtsZ-YFP foci in the cells expressing only

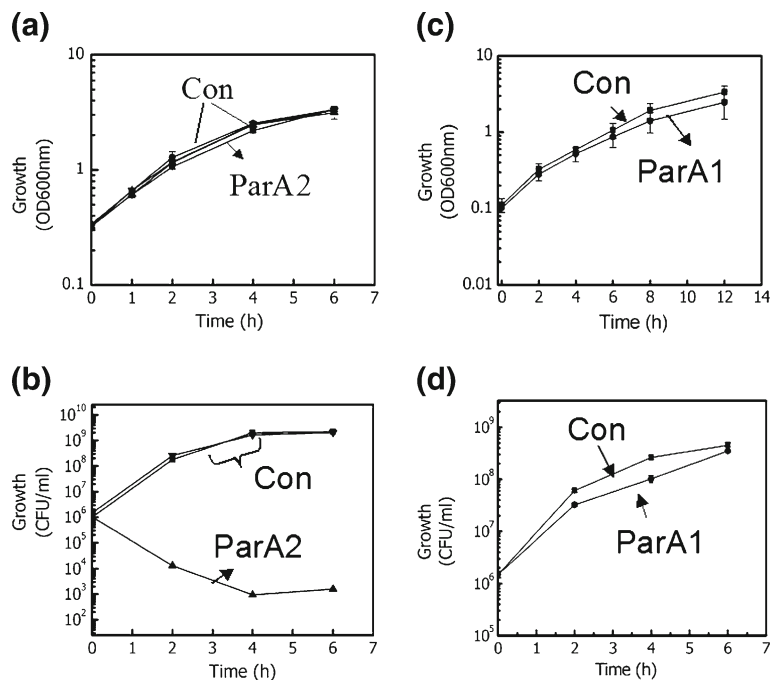


Figure 4. Effect of ParA2 expression on growth characteristics of *E. coli*. *E. coli* cells harbouring expression vector pAMCYAN (Con, -■- and -●-) and plasmid expressing ParA2 (ParA2, -▲- and -▼-) were induced with IPTG (-▲- and -■-) and compared with uninduced cells (-▼- and -●-). The effect of ParA2 expression on optical density (A) and colony-forming units per milliliter was monitored (B). Similarly, *E. coli* cells harbouring vector (Con) and expressing ParA1 (ParA1) were induced with IPTG and optical density at 600 nm (C) and colony-forming units (D) were monitored.

FtsZ-YFP was almost in mid cell and the average number of FtsZ-YFP foci per cell was ~ 1.0 . On the other hand, the cells expressing both ParA2 and FtsZ-YFP concurrently showed random positioning of FtsZ-YFP foci through the cells and the average number of such foci per cell was ~ 6.0 (figure 6). These results indicated that ParA2 over-expression *per se* could affect the productive pattern of FtsZ localization and eventually cytokinesis.

3.4 ParA2 complemented *SlmA* phenotype in *E. coli*

Binding of ParA2 with nucleoid and its effect on inhibition of cell division are the functions known also for nucleoid occlusion proteins such as SlmA in *E. coli* (Bernhardt and de Boer 2005) and 'Noc' in *Bacillus subtilis* (Wu and Errington 2004). These proteins are known to inhibit cell division by bringing nucleoid occlusion to the vicinity of FtsZ ring formation. Therefore, the possibility of ParA2 inhibiting cell division either by nucleoid occlusion or by affecting DNA replication and genome segregation could be hypothesized. ParA2 was expressed in *E. coli* strain TB85 ($\Delta slmA$) and *E. coli* strain TB86 ($\Delta minCDE \Delta slmA$) cells, and the effect of ParA2 on growth characteristics of these mutants were examined. The *slmA* mutant expressing ParA2 grew similar to mutant control, while ParA2 could help *slmA minCDE*

double mutant to recover its growth defect in rich medium (figure 7A) and produce asymmetric cell division generating high frequency of minicells (figure 7B). Double mutants expressing ParA2 produced $19.24 \pm 2.12\%$ minicells as against $5.12 \pm 1.26\%$ in control without ParA2. Asymmetric cell division has been observed in *E. coli* cells lacking MinCDE system (Lutkenhaus 2007). This indicated that ParA2 expression could make *slmA minCDE* double mutants similar to *minCDE* single mutants, implying the complementation of SlmA loss in the double mutant. These results may, therefore, suggest that ParA2 effect on cell division is most likely by affecting genome compaction, a process integral to nucleoid occlusion mechanisms operated by two distinctly different proteins SlmA in *E. coli* and 'Noc' in *B. subtilis*.

4. Discussion

D. radiodurans exposed to non-permissive dose of γ radiation shows relatively longer lag phase in the growth. During this period, the transcript levels of both divisome components and genome partitioning (Par) proteins do not change significantly (Liu *et al.* 2003; Tanaka *et al.* 2004). Although the composition and architecture of the cell wall and cell membrane in *D. radiodurans* (Baumeister *et al.* 1981; Thompson and Murray 1981), *B. subtilis* (Rogers, 1970) and *E. coli* (Lugtenberg and

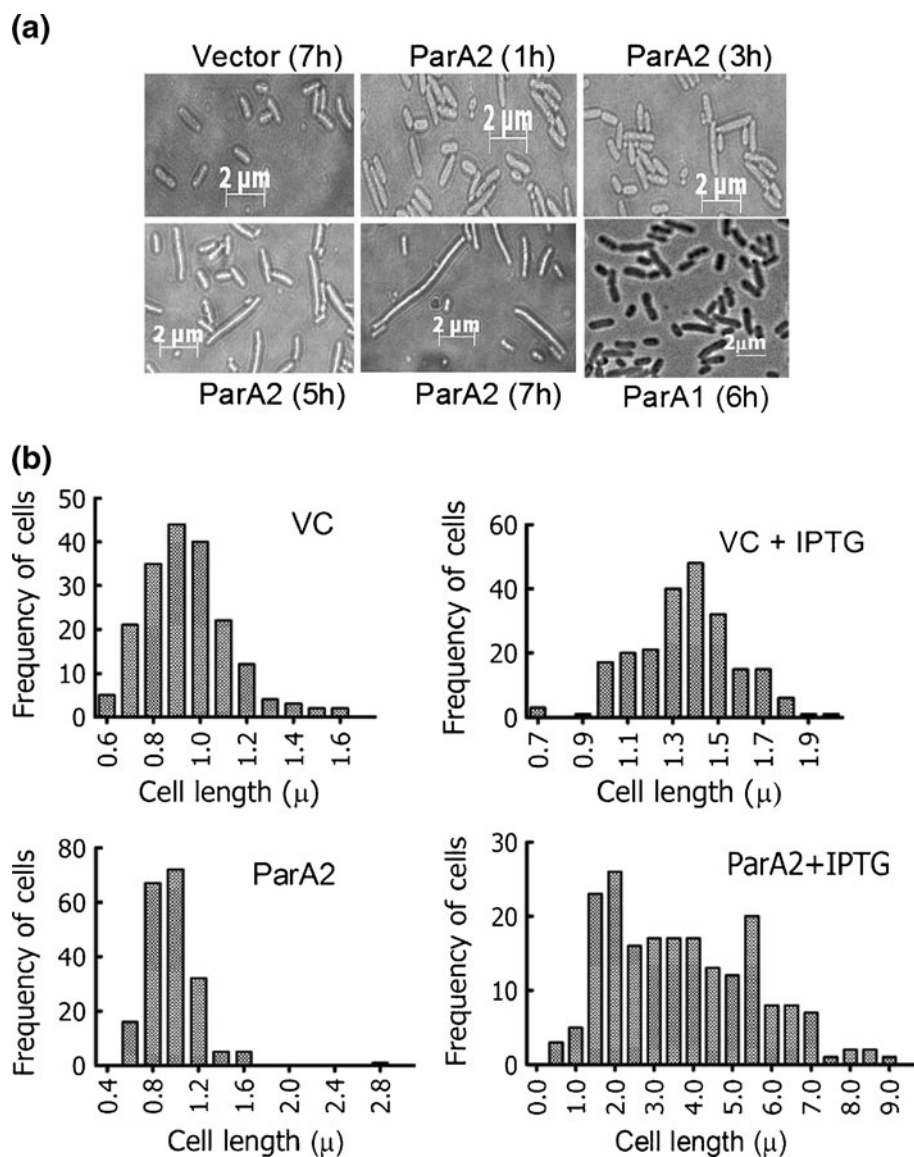


Figure 5. Effect of ParA2 expression on cell morphology of *E. coli*. *E. coli* cells harbouring pAMCYAN (vector) and expressing ParA2 (ParA2) and ParA1 were induced with IPTG for different time periods (as shown within parenthesis) and observed under a microscope (A). Similarly, *E. coli* cells harbouring pAMCYAN (VC) and pA2CFP (ParA2) were grown in absence (VC and ParA2) and presence of IPTG (VC+IPTG and ParA2 +IPTG) for 9 h and cells were imaged. The length of ~100 cells per sample was measured by Axiovision rel 4.8 software and the frequency of cells showing different sizes were calculated using Graphpad Prism 5 software (B).

Van 1983) are different, the divisome components in these bacteria are highly conserved at least at the levels of their primary sequences. ParA2 is found to be a DNA-binding protein *in vitro* and localizes with nucleoid *in vivo*. ParA2 expression also inhibits cell division and induces mislocalization of FtsZ-YFP throughout elongated cells of *E. coli*. Therefore, the possibility of ParA2's nucleoid binding activity contributing to cell division inhibition was hypothesized, and its expression on cellular lethality either by affecting DNA metabolism and/or by working like SlmA was checked. ParA2 expression did

not pose further lethality in wild-type *E. coli* lacking SlmA, which could have been anticipated if this protein had indiscriminately affected DNA replication and genome segregation in *E. coli*. However, the possibility of ParA2 regulating genome segregation in the presence of cognate ParB protein in its native host cannot be ruled out and is being investigated independently. Cellular lethality of ParA2 expressing in wild-type *E. coli*, which is already expressing indigenous copy of SlmA, could be due to increased dose effect on the common functions performed by both SlmA and ParA2. A similar

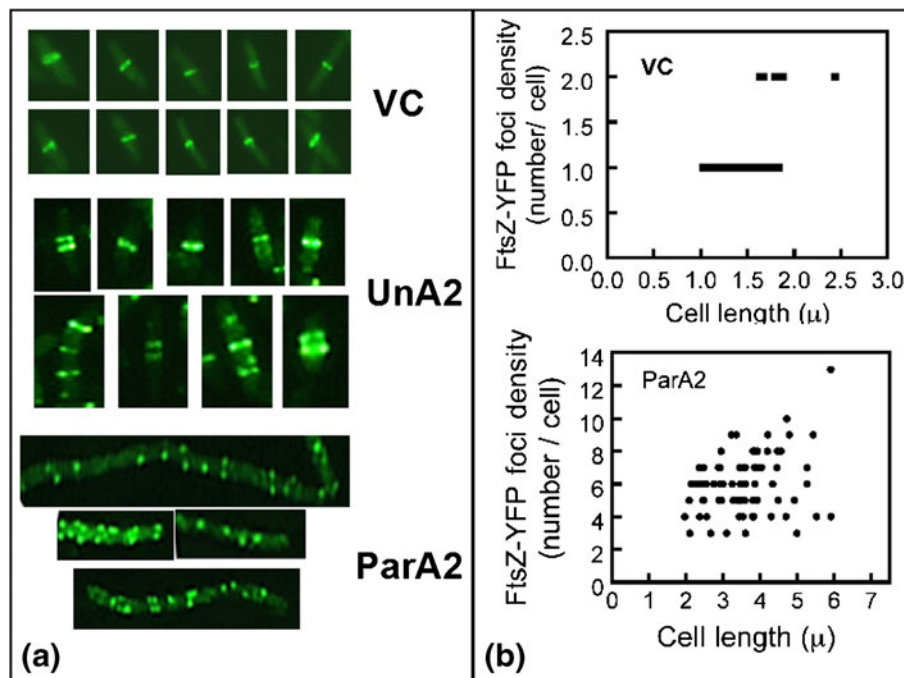


Figure 6. Effect of ParA2 expression on FtsZ ring formation in *E. coli*. The cells expressing FtsZ-YFP under *araBAD* promoter on pLAU85 were further transformed with pET28a (+) (A) and pETA2 (B, C) plasmids. These cells were induced with 0.005% arabinose and further grown in the absence (B) and presence (A, C) of IPTG. Cells were imaged using Axioimager microscope for the expression of YFP was shown. Slices obtained from the images taken at 2 μ m scale are shown in supplementary figure 4. Cell length and number of FtsZ-YFP foci per *E. coli* cell grown in absence (VC) and presence of ParA2 (ParA2) were computed from 100 cells each and plotted as density of FtsZ-YFP foci in form of the number of foci /cells versus cell length.

phenotype was observed when SlmA was expressed on multicopy plasmid (Bernhardt and de Boer 2005). On the other hand, ParA2 expressing in *slmA*minCDE double mutants shows unequal cell division and produced higher frequency of minicells (figure 7B). *E. coli* cells defective in MinCDE proteins undergo asymmetric cell division at the poles, leading to formation of minicells (Lutkenhaus 2007). These results indicated that ParA2 could complement SlmA loss in double mutants. Recently, Cho and coworkers have shown that the purified SlmA could inhibit both GTPase activity and sedimentation characteristics of FtsZ *in vitro* (Cho *et al.* 2011). The similar effect of MipZ on FtsZ polymerization and Z ring formation was also reported earlier in *Caulobacter crescentus* (Thanbichler and Shapiro 2006). Since ParA2 is found to be evolutionarily closer to MipZ (figure 1A), the effect of ParA2 on FtsZ activity and sedimentation characteristics was checked. Remarkably, there was no effect of purified recombinant ParA2 on GTPase activity and the sedimentation characteristics of FtsZ up to 5-fold molar excess of ParA2 coincubated with FtsZ in the presence and absence of non-specific DNA (figure 8). Considering the diversity of the proteins regulating cell division and genome segregation in bacteria, this result did not surprise us. As we know, SlmA and ‘Noc’ proteins, which bring about nucleoid occlusion

in *E. coli* (Tonthat *et al.* 2011) and *Bacillus subtilis* (Wu and Errington 2004), are also different in terms of their amino acid sequences and mechanism of action. For example, SlmA is shown to affect FtsZ polymerization and GTPase activity *in vitro* while such effects of ‘Noc’ has not been reported (Cho *et al.* 2011). Also, amongst the SlmA, ‘Noc’ and MipZ proteins, which regulate bacterial cell division, the SlmA and Noc are sequence-specific DNA-binding proteins while MipZ interacts with the chromosome of *Caulobacter* non-specifically (Thanbichler and Shapiro 2006). Although the precise mechanism underlying ParA2 inhibition of cell division could not be outlined, mechanistically it seems to be different from SlmA and MipZ, at least in respect to its direct interaction with FtsZ. Interestingly, the purified recombinant ParA2 by itself showed sedimentation at centrifugal force equivalent to 20000g, which increased further in the presence of dsDNA and ATP. However, when this mixture was co-incubated with cognate ParB2, the amount of ParA2 in the pellet had decreased significantly (data not shown), indicating that ParB2 could destabilizes the ParA2–dsDNA interaction. Therefore, the possibility of ParA2 affecting bacterial cell division by stabilizing genome compaction *albeit* in the absence of cognate ParB2 cannot be ruled out. Since ParA2 did not affect FtsZ characteristics *in solution*,

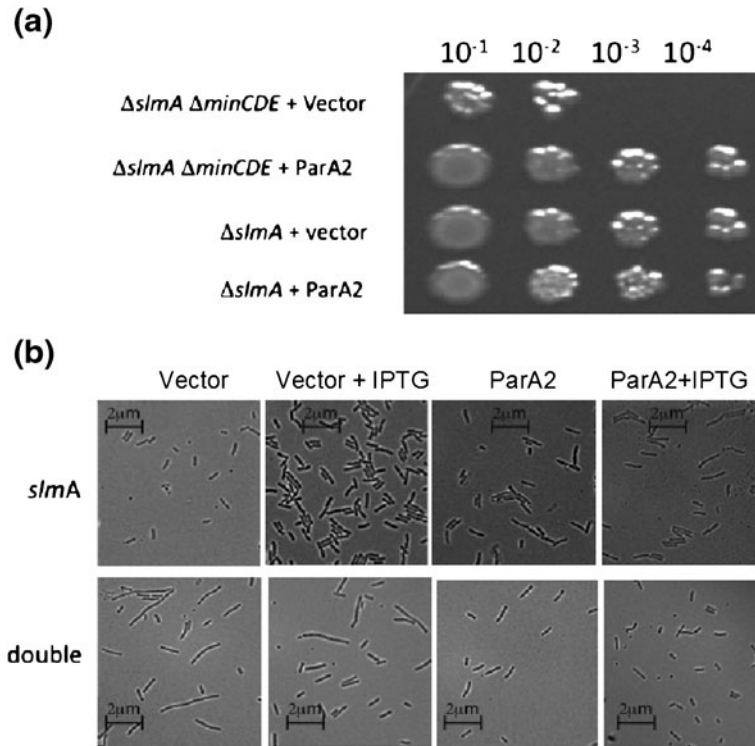


Figure 7. Functional complementation studies with *E. coli* mutants. The $\Delta slmA$ and $\Delta slmA \Delta minCDE$ ($\Delta slmA \Delta minCDE$ / double) mutants of *E. coli* were transformed with pAMCYAN (vector) and pA2CFP (ParA2) and grown in the presence and absence of IPTG for 4 h. The 2 μ L of IPTG induced cells were spotted in different dilutions and growth was recorded (A). Similarly, the both vector containing cells and ParA2 expressing cells were grown in absence (vector, ParA2) and presence of IPTG (vector + IPTG, ParA2 + IPTG) were observed under microscope (B).

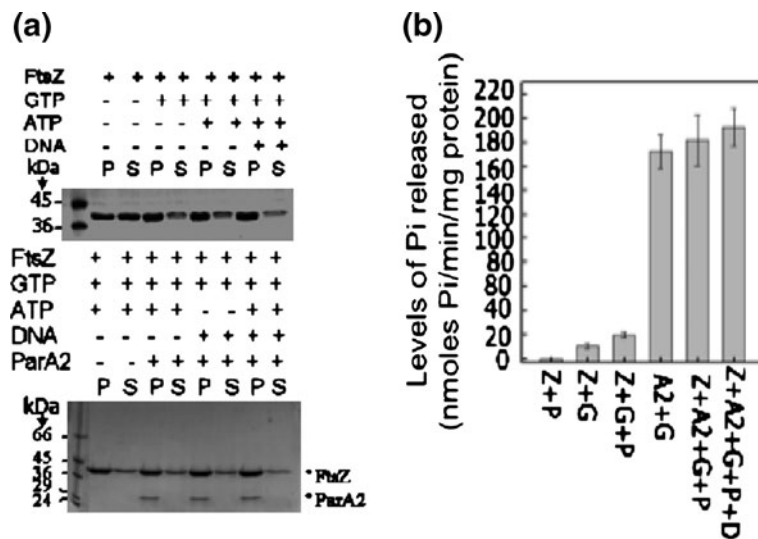


Figure 8. Effect of ParA2 on polymerization characteristics and GTPase activity of FtsZ from *D. radiodurans*. (A) Sedimentation analysis of FtsZ was checked under standard assay conditions in the presence of the different combination of ATP, GTP and DNA and without ParA2 (upper panel) and with ParA2 (lower panel). Pellets and supernatants were analysed on SDS-PAGE and the distributions of FtsZ in the pellet and supernatant fractions were checked in respective samples by coomassie staining. (B) Purified FtsZ (Z) was incubated with ATP (P), GTP (G), ParA2 (A2) and dsDNA (D) in different combinations and release of inorganic phosphate from GTP/ATP was measured as described in section 2.

which SlmA and MipZ do, and ParA2 was found to be a non-specific DNA-binding protein like MipZ while SlmA and 'Noc' bind to the specific sites on nucleoids, the possibility of ParA2 regulating bacterial cell division and FtsZ localization through nucleoid compaction by an as-yet uncharacterized mode of action may be suggested.

Acknowledgements

We thank Dr SK Apte, for his technical comments on this work. We are grateful to Professor Dhruba K Chatteraj, NCI, NIH, for FtsZ-YFP constructs, and Dr Bhavani Shankar for her help in fluorescence microscopy studies.

Reference

- Adams DW and Errington J 2009 Bacterial cell division: assembly, maintenance and disassembly of the Z ring. *Nat. Rev. Microbiol.* **7** 642–653
- Battista J R 2000 Radiation resistance: the fragments that remain. *Curr. Biol.* **10** R204–R205
- Battista JR, ParK MJ and McLemore AE 2001 Inactivation of two homologues of proteins presumed to be involved in the desiccation tolerance of plants sensitizes *Deinococcus radiodurans* R1 to desiccation. *Cryobiology* **43** 133–139
- Baumeister W, Kubler O and Zingsheim HP 1981 The structure of the cell envelope of *Micrococcus radiodurans* as revealed by metal shadowing and decoration. *J. Ultrastruct. Res.* **75** 60–71
- Bernhardt TG and de Boer PA 2005 SlmA, a nucleoid-associated, FtsZ binding protein required for blocking septal ring assembly over chromosomes in *E. coli*. *Mol. Cell.* **18** 555–564
- Blasius M, Sommer S and Hubscher U 2008 *Deinococcus radiodurans*: what belongs to the survival kit? *Crit. Rev. Biochem. Mol. Biol.* **43** 221–238
- Charaka VK and Misra HS 2012 Functional characterization of chromosome I partitioning system in *Deinococcus radiodurans* for its role in genome segregation. *J. Bacteriol.* **194** 5739–5748
- Cho H, McManus HR, Dove SL and Bernhardt TG 2011 Nucleoid occlusion factor SlmA is a DNA-activated FtsZ polymerization antagonist. *Proc. Natl. Acad. Sci. USA* **108** 3773–3778
- Cox MM and Battista JR 2005 *Deinococcus radiodurans* - the consummate survivor. *Nat. Rev. Microbiol.* **3** 882–892
- Dajkovic A, Mukherjee A and Lutkenhaus J 2008 Investigation of regulation of FtsZ assembly by SulA and development of a model for FtsZ polymerization. *J. Bacteriol.* **190** 2513–2526
- Daly MJ, Gaidamakova EK, Matrosova VY, Vasilenko A, Zhai M, Venkateswaran A, Hess M, Omelchenko MV, Kostandarithes HM, Makarova KS, Wackett LP, Fredrickson JK and Ghosal D 2004 Accumulation of Mn(II) in *Deinococcus radiodurans* facilitates gamma-radiation resistance. *Science* **306** 1025–1028
- Das AD and Misra HS 2011 Characterization of DRA0282 from *Deinococcus radiodurans* for its role in bacterial resistance to DNA damage. *Microbiology* **157** 2196–2205
- Erickson HP, Anderson DE and Osawa M 2010 FtsZ in bacterial cytokinesis: cytoskeleton and force generator all in one. *Microbiol. Mol. Biol. Rev.* **74** 504–528
- Geladopoulos TP, Sotiroudis TG and Evangelopoulos AE 1991 A Malachite Green Colorimetric Assay for protein phosphatase activity. *Anal. Biochem.* **192** 112–116
- Kawai Y, Moriya S and Ogasawara N 2003 Identification of a protein, YneA, responsible for cell division suppression during the SOS response in *Bacillus subtilis*. *Mol. Microbiol.* **47** 1113–1122
- Kota S, Kumar VC and Misra HS 2010 Characterization of an ATP-regulated DNA-processing enzyme and thermotolerant phosphoesterase in the radioresistant bacterium *Deinococcus radiodurans*. *Biochem. J.* **431** 149–157
- Lau IF, Filipe SR, Soballe B, Okstad OA, Barre FX and Sherratt DJ 2003 Spatial and temporal organization of replicating *Escherichia coli* chromosomes. *Mol. Microbiol.* **49** 731–743
- Liu Y, Zhou J, Omelchenko MV, Beliaev AS, Venkateswaran A, Stair J, et al 2003 Transcriptome dynamics of *Deinococcus radiodurans* recovering from ionizing radiation. *Proc. Natl. Acad. Sci. USA* **100** 4191–4196
- Lugtenberg B and Van AL 1983 Molecular architecture and functioning of the outer membrane of *Escherichia coli* and other gram-negative bacteria. *Biochim. Biophys. Acta.* **737** 51–115
- Lutkenhaus J 2007 Assembly dynamics of the bacterial MinCDE system and spatial regulation of the Z ring. *Annu. Rev. Biochem.* **76** 539–562
- Makarova KS, Aravind L, Wolf YI, Tatusov RL, Minton KW, Koonin EV and Daly MJ 2001 Genome of the extremely radiation-resistant bacterium *Deinococcus radiodurans* viewed from the perspective of comparative genomics. *Microbiol. Mol. Biol. Rev.* **65** 44–79
- Misra HS, Khairnar NP, Kota S, Shrivastava S, Joshi VP and Misra HS 2006 An Exonuclease I sensitive DNA repair pathway in *Deinococcus radiodurans*: a major determinant of radiation resistance. *Mol. Microbiol.* **59** 1308–1316
- Misra HS, Rajpurohit YS and Khairnar NP 2012 Pyrroloquinoline-quinone and its versatile roles in biological processes. *J. Biosci.* **37** 313–25
- Narumi I, Satoh K, Kikuchi M, Funayama T, Yanagisawa T, Kobayashi Y, Watanabe H and Yamamoto K 2001 The LexA protein from *Deinococcus radiodurans* is not involved in RecA induction following gamma irradiation. *J. Bacteriol.* **183** 6951–6956
- Norman A, Hestbjerg HL and Sorensen SJ 2005 Construction of a ColD cda promoter-based SOS-green fluorescent protein whole-cell biosensor with higher sensitivity toward genotoxic compounds than constructs based on *recA*, *umuDC*, or *sulA* promoters. *Appl. Environ. Microbiol.* **71** 2338–2346
- Rajpurohit YS, Gopalakrishnan R and Misra HS 2008 Involvement of a protein kinase activity inducer in DNA double strand break repair and radioresistance of *Deinococcus radiodurans*. *J. Bacteriol.* **190** 3948–3954
- Rogers HJ 1970 Bacterial growth and the cell envelope. *Bacteriol. Rev.* **34** 194–214
- Sambrook J and Russell DW 2001 Molecular Cloning: A laboratory manual 3rd edition (Cold Spring Harbor, NY: Cold Spring Harbor Laboratory Press)
- Schaefer M, Schmitz C, Facius R, Horneck G, Milow B, Funken KH and Ortner J 2000 Systematic study of parameters influencing the action of Rose Bengal with visible light on bacterial

- cells: comparison between the biological effect and singlet-oxygen production. *Photochem. Photobiol.* **71** 514–523
- Slade D and Radman M 2011 Oxidative stress resistance in *Deinococcus radiodurans*. *Microbiol. Mol. Biol. Rev.* **75** 133–191
- Tanaka M, Earl AM, Howell HA, Park MJ, Eisen JA, Peterson SN and Battista JR 2004 Analysis of *Deinococcus radiodurans*'s transcriptional response to ionizing radiation and desiccation reveals novel proteins that contribute to extreme radioresistance. *Genetics* **168** 21–33
- Thanbichler M and Shapiro L 2006 MipZ, a spatial regulator coordinating chromosome segregation with cell division in *Caulobacter*. *Cell* **126** 147–162
- Thompson BG and Murray RG 1981 Isolation and characterization of the plasma membrane and the outer membrane of *Deinococcus radiodurans* strain Sark. *Can. J. Microbiol.* **27** 729–734
- Tian B and Hua Y 2010 Carotenoid biosynthesis in extremophilic *Deinococcus-Thermus* bacteria. *Trends Microbiol.* **18** 512–520
- Tonthat NK, Arold ST, Pickering BF, Van Dyke MW, Liang S, Lu Y and Beuria TK 2011 Molecular mechanism by which the nucleoid occlusion factor, SlmA, keeps cytokinesis in check. *EMBO J.* **30** 154–164
- Walker GC 1996 The SOS Response of *Escherichia coli*; in *Escherichia coli* and *Salmonella*: Cellular and molecular biology (eds) FC Neidhardt, R Curtiss III, JL Ingraham, ECC Lin, KB Low, B Magasanik, WS Reznikoff, M Riley, M Schaechter and HE Umbarger (Washington DC:ASM Press) pp 1400–1416
- Weiss DS, Chen JC, Ghigo JM, Boyd D and Beckwith J 1999 Localization of FtsI (PBP3) to the septal ring requires its membrane anchor, the Z ring, FtsA, FtsQ, and FtsL. *J. Bacteriol.* **181** 508–520
- White O, Eisen JA, Heidelberg JF, Hickey EK, Peterson JD, Dodson RJ, et al 1999 Genome sequence of the radioresistant bacterium *Deinococcus radiodurans* R1. *Science* **286** 1571–1577
- Wu LJ and Errington J 2004 Coordination of cell division and chromosome segregation by a nucleoid occlusion protein in *Bacillus subtilis*. *Cell* **117** 915–925
- Zahradka K, Slade D, Bailone A, Sommer S, Averbek D, Petranovic M, Lindner AB and Radman M 2006 Reassembly of shattered chromosomes in *Deinococcus radiodurans*. *Nature* **443** 569–573
- Zusman DR, Carbonell A and Haga JY 1973 Nucleoid Condensation and Cell Division in *Escherichia coli* MX74T2 ts52 After Inhibition of Protein Synthesis. *J. Bacteriol.* **115** 1167–1178

MS received 18 February 2013; accepted 27 May 2013

Corresponding editor: MANJULA REDDY